Electronic structure and spontaneous internal field around nonmagnetic impurities in spin-triplet chiral *p*-wave superconductors

Mitsuaki Takigawa*
Department of Applied Physics, Hokkaido University, Sapporo 060-8628, Japan

Masanori Ichioka
Department of Physics, Okayama University, Okayama 700-8530, Japan

Kazuhiko Kuroki
Department of Applied Physics and Chemistry, University of Electro-Communications, Chofu, Tokyo 182-8585, Japan

Yukio Tanaka
Department of Material Science and Technology, Nagoya University, Nagoya 464-8603, Japan
(Received 5 April 2005; revised manuscript received 6 September 2005; published 6 December 2005)

The electronic structure around an impurity in spin-triplet *p*-wave superconductors is studied by the Bogoliubov–de Gennes theory on a tight-binding model, where we have chosen $\sin p_x + i \sin p_y$-wave or $\sin(p_x+p_y)+i\sin(-p_x+p_y)$-wave states, which are considered to be candidates for the pairing state in Sr_2RuO_4. We calculate the spontaneous current and the local density of states around the impurity and discuss the difference between the two types of pairing. We propose that it is possible to discriminate the two pairing states by studying the spatial dependence of the magnetic field around a pair of impurities.

DOI: 10.1103/PhysRevB.72.224501 PACS number(s): 74.25.Jb, 74.20.Rp, 73.20.Hb, 74.70.Pq

I. INTRODUCTION

The discovery of superconductivity in Sr_2RuO_4 by Maeno *et al.*[1] has activated the field of spin-triplet superconductivity,[2] which has been studied for more than 30 years.[3,4] There are many studies suggesting that spin-triplet pairing is realized in Sr_2RuO_4.[5–11] The presence of a spontaneous magnetic field suggested from the μSR experiment is consistent with a chiral superconductivity with a broken time reversal symmetry (BTRSS).[12] Tunneling spectroscopy with a zero bias conductance peak[13] is also consistent with spin-triplet pairing with BTRSS.[14]

Theoretically, several pairing states and/or microscopic mechanisms for spin-triplet *p*-wave pairing in Sr_2RuO_4 have been proposed.[15–20] Although there are three bands in Sr_2RuO_4, it is possible to consider the essence of the superconducting property only by considering the quasi-two-dimensional γ band. For simplicity, we classify the pairings for Sr_2RuO_4 as two types, which are qualitatively consistent with experiments of specific heat.[21] The first type is the $\sin p_x + i \sin p_y$ wave proposed by Miyake and Narikiyo (MN),[15] where Cooper pairs are formed between nearest-neighbor sites. The second one is the $\sin(p_x+p_y)+i\sin(-p_x+p_y)$-wave state proposed by Arita, Onari, Kuroki, and Aoki (AOKA),[17] where the pairs are formed between next-nearest-neighbor sites. The pairing which has been proposed based on the third-order perturbation theory[18,19] has more higher harmonics, where the most dominant component is the $\sin(p_x+p_y)+i\sin(-p_x+p_y)$-wave pairing. In the following, we call $\sin p_x + i \sin p_y$-wave pairing and $\sin(p_x+p_y)+i\sin(-p_x+p_y)$-wave pairing MN-type pairing, and AOKA-type, respectively. The discrimination of the MN-type and the AOKA-type pairings is important because it is strongly related to the study of the superconducting properties and the pairing mechanism of Sr_2RuO_4. One of the remarkable differences of the two pairing states is the winding number of the pairing function when we trace its phase along the γ-band Fermi surface.[22] The winding number is one in the MN-type pairing; three in the AOKA-type pairing. It is interesting to propose a new idea to discriminate these two pairings having different topological characters.

The aim of this paper is to propose that the experimental observation of the electronic properties and the internal field around an impurity can be used to discriminate the two pairing states. As shown in recent experiments by Lupien *et al.*, it is possible to observe the local density of states (LDOS) in Sr_2RuO_4 with high accuracy.[23] There are some works studying the modulation of the electronic structure around the magnetic and/or nonmagnetic impurities in superconductors.[24–26] From the electronic structures modulated around impurities, we can obtain the features of the electronic states in the superconductor, including the anisotropies of the pairing and the Fermi surface. The action of the nonmagnetic impurities cannot be neglected in the bulk properties of the unconventional superconductors, while it is absent in the conventional superconductors. Among the unconventional superconductors, when the pairing is BTRSS, spontaneous circular current is induced around a nonmagnetic impurity.[27,28] This may be a possible origin of the spontaneous magnetic field observed in the μSR experiment.[12] The induced currents and magnetic fields do not appear around nonmagnetic impurities in the conventional and unconventional superconductors with time reversal symmetry.

After describing our formulation by the Bogoliubov–de Genens (BdG) theory in Sec. II, we study the single impurity

state in Sec. III, calculating the LDOS and spontaneous magnetic field around a nonmagnetic impurity to discuss the difference between the two pairings; NM type and AOKA type. In Sec. IV, we consider the case of two nonmagnetic impurities, which shows eminent difference of two pairings. The last section is devoted to the summary.

II. BOGOLIUBOV-de GENNES THEORY

We start from the tight-binding model with nonlocal spin-triplet p-wave pairing interactions[22] to study the electronic states around an impurity. The Hamiltonian is given by

$$\mathcal{H} = \sum_{j,i,\sigma} K_{ij} a^{\dagger}_{j,\sigma} a_{i,\sigma} + \sum_{i,j} (\Delta_{ji} a^{\dagger}_{j,\uparrow} a^{\dagger}_{i,\downarrow} + \text{c.c.}), \tag{1}$$

where $K_{i,j} = -t_{i,j} - (\mu + \delta\mu_{\text{imp},i})\delta_{i,j}$, and we assume that the d vector of the pair potential is parallel to the z axis in the spin space. We set $t_{i,j} = t$, $(-0.4t)$ for the transfer between nearest- (second nearest) neighbor sites in the two-dimensional square lattice of Ru atoms. The sites are labeled $i = (i_x, i_y)$. We neglect the vector potential due to the induced magnetic field in the transfer term, since this contribution is small in typical type-II superconductors. The energy and the temperature are scaled by t throughout this paper. The chemical potential μ, which depends on the temperature, is tuned so that the density of electron is fixed at $\langle n \rangle = \frac{4}{3}$. This reproduces the Fermi surface topology of the γ sheet in Sr_2RuO_4.[22]

We consider a system with a square unit cell of $N_r \times N_r$ sites. Here, we show the results for $N_r = 31$. An impurity is located at the center of the unit cell. Then, within 31×31 sites, a nonmagnetic impurity is located at the center site $i = (16, 16)$ for the single impurity case, or two impurities are located at $i = (15, 15)$ and (16, 16) in the case of two impurities. At the impurity sites, we assume that Ru atoms are switched with the impurities and introduce the impurity potential $\delta\mu_{\text{imp},i}$ at the impurity site, as is the standard method for treating nonmagnetic impurities. We consider the case when $\delta\mu_{\text{imp},i} = -17.5t$, which is a strong impurity potential, as a Ti doped case, and the wave functions are almost zero at the impurity site. In order to avoid the artificial effects caused by the discrete energy levels of a finite system, our calculations are performed in the system of $N_k \times N_k$ unit cells with a periodic boundary condition based on the concept of the Bloch state, so that the energy spectrum is almost continuous in this large system.

Using the Bogoliubov transformation

$$\begin{pmatrix} a_{i,\uparrow} \\ a^{\dagger}_{i,\downarrow} \end{pmatrix} = \sum_{\epsilon} \begin{pmatrix} u_{\epsilon}(\mathbf{r}_i) & u'_{\epsilon}(\mathbf{r}_i) \\ v_{\epsilon}(\mathbf{r}_i) & v'_{\epsilon}(\mathbf{r}_i) \end{pmatrix} \begin{pmatrix} \gamma_{\uparrow,\epsilon} \\ \gamma^{\dagger}_{\downarrow,\epsilon} \end{pmatrix}, \tag{2}$$

we obtain the BdG equation

$$\sum_{i} \begin{pmatrix} K_{ji} & \Delta_{ji} \\ \Delta^{\dagger}_{ji} & -K^{*}_{ji} \end{pmatrix} \begin{pmatrix} u_{\epsilon}(\mathbf{r}_i) \\ v_{\epsilon}(\mathbf{r}_i) \end{pmatrix} = E_{\epsilon} \begin{pmatrix} u_{\epsilon}(\mathbf{r}_j) \\ v_{\epsilon}(\mathbf{r}_j) \end{pmatrix}, \tag{3}$$

where $\Delta^{\dagger}_{ji} = \Delta^{*}_{ij}$. From the BdG equation with eigenenergy $-E_{\epsilon}$, we obtain wave functions $[u'_{\epsilon}(\mathbf{r}_j), v'_{\epsilon}(\mathbf{r}_j)]$. Using the relation $\Delta_{ji} = -\Delta_{ij}$ in the triplet pairing, we see that $[u'_{\epsilon}(\mathbf{r}_j), v'_{\epsilon}(\mathbf{r}_j)] = [v^{*}_{\epsilon}(\mathbf{r}_j), u^{*}_{\epsilon}(\mathbf{r}_j)]$. We note that in the singlet pairing $[u'_{\epsilon}(\mathbf{r}_j), v'_{\epsilon}(\mathbf{r}_j)] = [-v^{*}_{\epsilon}(\mathbf{r}_j), u^{*}_{\epsilon}(\mathbf{r}_j)]$, since $\Delta_{ji} = \Delta_{ij}$.

Introducing the quasimomentum

$$\mathbf{k} = \frac{2\pi}{aN_rN_k}(l_x, l_y), \quad (l_x, l_y = 1, \cdots, N_k) \tag{4}$$

with the lattice constant a, we can write the wave functions in Eq. (3) as the Bloch states;

$$u_{\epsilon}(\mathbf{r}) = \tilde{u}_{\mathbf{k},\epsilon_{\mathbf{k}}}(\mathbf{r}) e^{i\mathbf{k}\cdot\mathbf{r}}, \quad v_{\epsilon}(\mathbf{r}) = \tilde{v}_{\mathbf{k},\epsilon_{\mathbf{k}}}(\mathbf{r}) e^{i\mathbf{k}\cdot\mathbf{r}}. \tag{5}$$

The eigenstate ϵ in Eq. (3) can be labeled by the quasimomentum $\mathbf{k}$ and the eigenenergy $\epsilon_{\mathbf{k}}$ given $\mathbf{k}$. Since the wave functions $\tilde{u}_{\mathbf{k},\epsilon_{\mathbf{k}}}$ and $\tilde{v}_{\mathbf{k},\epsilon_{\mathbf{k}}}$ satisfy the periodic boundary condition for a unit cell with $N_r \times N_r$ site, we numerically solve the eigenvalue problem of the $2N_r^2 \times 2N_r^2$ matrix in Eq. (3) with the substitution of Eq. (5) in a unit cell for each $\mathbf{k}$, and obtain the wave functions $u_{\epsilon}(\mathbf{r})$, $v_{\epsilon}(\mathbf{r})$ and the eigenenergies E_{ϵ}. We typically consider the case $g_{z,ji} = -t$ at a low temperature $T = 0.01t$.

The self-consistent condition for the spin-triplet pair potential is

$$\Delta_{ij} = g_{z,ji}(\langle a_{j\downarrow} a_{i\uparrow} \rangle + \langle a_{j\uparrow} a_{i\downarrow} \rangle) \tag{6}$$

with

$$\langle a_{j\downarrow} a_{i\uparrow} \rangle = \sum_{\epsilon} v^{*}_{\epsilon}(\mathbf{r}_j) u_{\epsilon}(\mathbf{r}_i) f(E_{\epsilon}), \tag{7}$$

$$\langle a_{j\uparrow} a_{i\downarrow} \rangle = \sum_{\epsilon} u_{\epsilon}(\mathbf{r}_j) v^{*}_{\epsilon}(\mathbf{r}_i) f(-E_{\epsilon}), \tag{8}$$

where $f(E_{\epsilon}) = \langle \gamma^{\dagger}_{\uparrow,\epsilon} \gamma_{\uparrow,\epsilon} \rangle$ is the Fermi distribution function, and $g_{z,ji}$ is the spin-triplet pairing interaction. The summation for ϵ indicates that we add all contributions from eigenstates with both positive and negative eigenenergies. The orbital part of the pair potential at each site i can be decomposed into sin p_x- and sin p_y-components as

$$\Delta_{p_x}(\mathbf{r}_i) = (\Delta_{i,i+\hat{x}} - \Delta_{i,i-\hat{x}})/2, \tag{9}$$

$$\Delta_{p_y}(\mathbf{r}_i) = (\Delta_{i,i+\hat{y}} - \Delta_{i,i-\hat{y}})/2 \tag{10}$$

as $g_{z,ij}$ is nonzero for only the nearest-neighbor (NN) site pair in the MN-type pairing. For sin $p_x \pm i$ sin p_y-wave superconductivity, we define the pair potential as $\Delta_{\pm}(\mathbf{r}_i) \equiv \Delta_{p_x}(\mathbf{r}_i) \pm i\Delta_{p_y}(\mathbf{r}_i)$. When the pair potential is uniform, this BdG formulation is reduced to the conventional theory for p-wave superconductors with the MN-type pairing functions, which has an anisotropic gap $(\sin^2 p_x + \sin^2 p_y)^{1/2}$. In the AOKA-type pairing case, as $g_{z,ij}$ is nonzero for only the second nearest site pairs, the pair potential $\Delta'_{\pm}(\mathbf{r}_i)$ is defined by $\Delta_{i,i+(\hat{x}+\hat{y})}$ and $\Delta_{i,i+(-\hat{x}+\hat{y})}$ instead of $\Delta_{i,i+\hat{x}}$ and $\Delta_{i,i+\hat{y}}$. By alternately solving Eqs. (3) and (6), we obtain the self-consistent solution for the impurity state.

To investigate the electronic structure around the impurity, we calculate the LDOS at the ith site as

$$N(E, \mathbf{r}_i) = \sum_{\epsilon} \{ |u_{\epsilon}(\mathbf{r}_i)|^2 \, \delta(E - E_{\epsilon}) + |v_{\epsilon}(\mathbf{r}_i)|^2 \, \delta(E + E_{\epsilon}) \}, \tag{11}$$

using self-consistently obtained $u_{\epsilon}(\mathbf{r}_i)$, $v_{\epsilon}(\mathbf{r}_i)$, and E_{ϵ}.

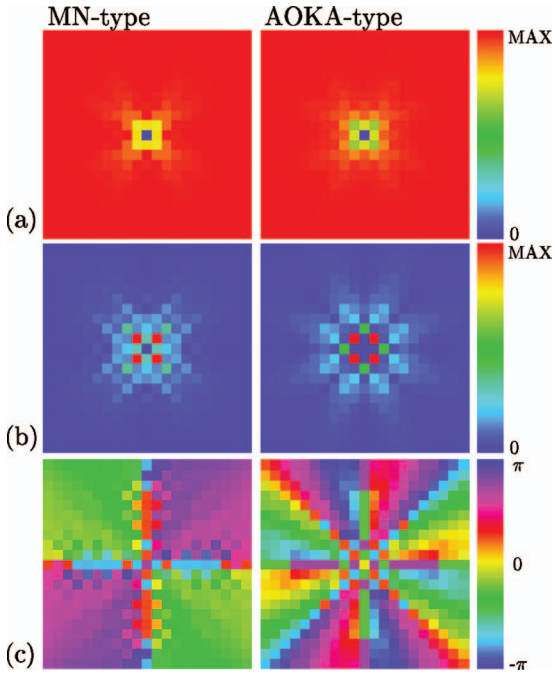

FIG. 1. (Color) Spatial structure of the pairing potential for the MN-type (left panels) and the AOKA-type (right panels) pairings. We show a region consisting of 21×21 sites with the impurity located at the center. (a) Amplitude of the dominant chiral component, $|\Delta_+(\mathbf{r})|$ or $|\Delta'_+(\mathbf{r})|$. (b) Amplitude of the induced opposite chiral component, $|\Delta_-(\mathbf{r})|$ or $|\Delta'_-(\mathbf{r})|$. (c) Phase structure of the induced component, $\mathrm{Arg}\Delta_-(\mathbf{r})$ or $\mathrm{Arg}\Delta'_-(\mathbf{r})$. The phase of the dominant chiral component is almost uniform.

The supercurrent $\mathbf{j}(\mathbf{r})$ in the tight-binding model is calculated as

$$j_{\hat{e}}(\mathbf{r}_i) = 2|e|c\ \mathrm{Im}\left(t_{i+\hat{e},i}\sum_{\sigma}\langle a^{\dagger}_{i+\hat{e},\sigma}a_{i,\sigma}\rangle\right)$$
$$= 2|e|c\ \mathrm{Im}\left(t_{i+\hat{e},i}\sum_{\epsilon}[u^{*}_{\epsilon}(\mathbf{r}_{i+\hat{e}})u_{\epsilon}(\mathbf{r}_i)f(E_{\epsilon})\right.$$
$$\left.+\,v_{\epsilon}(\mathbf{r}_{i+\hat{e}})v^{*}_{\epsilon}(\mathbf{r}_i)(1-f(E_{\epsilon}))]\right) \qquad (12)$$

for the $\hat{e}$-direction bond ($\hat{e}=\pm\hat{x},\pm\hat{y}$) at site $\mathbf{r}_i$. The spontaneous current $j_{\hat{e}}(\mathbf{r}_i)$, induced around an impurity, circles around the impurity when time reversal symmetry is broken. From the current, we evaluate the spontaneous internal field $\mathbf{H}(\mathbf{r})$ through the Maxwell equation $\nabla\times\mathbf{H}=4\pi/c\ \mathbf{j}(\mathbf{r})$.

III. SINGLE IMPURITY

A. Order parameter around the impurity

First we study the properties around a single impurity, which is located at site (16,16), and compare the results of the MN-type and the AOKA-type pairing cases. Figure 1 shows the pair potential structure around the impurity for MN-type pairing and for AOKA-type pairing. The amplitude of the dominant chiral component (Δ_+ or Δ'_+ here) vanishes at the impurity site, and recovers within a few sites from the impurity, as shown in Fig. 1(a). On the other hand, the other component with opposite chirality (Δ_- or Δ'_-) is induced around the impurity, as shown in Fig. 1(b).

The phase structure of the induced component, shown in Fig. 1(c), has a remarkable difference between the two pairing cases, reflecting the winding along the Fermi surface. In the MN case, $\mathrm{Arg}\Delta_-$ has +2-windings at the impurity site, and −1-winding at four sites located eight sites away from the impurity along the vertical and the horizontal directions. In the AOKA case, $\mathrm{Arg}\Delta'_-$ has −6-windings at the impurity site, and +1-winding at four sites located on the diagonal directions in addition to +1-winding at four sites on the vertical and horizontal directions. Since the amplitude of the induced component vanishes at these winding center sites, $|\Delta'_-|$ is more suppressed around the impurity with −6-windings, and the tails of $|\Delta'_-|$ have a shape extending toward eight directions far from the impurity.

The special features of the impurity states in the superconductor with BTRSS come from two-component pair potential $\Delta_\pm(\Delta'_\pm)$ with positive and negative chirality (i.e., nonzero angular momentum of the Cooper pair). Around an impurity where the dominant chiral component is suppressed, there appears to be the opposite chiral component, which has phase winding around the impurity. Due to the phase winding, the supercurrent circles around the impurity and a spontaneous magnetic field appears. From the difference of the winding structure of the induced chiral component, there appears to be some differences in the spontaneous field distribution around the impurity between the MN-type and the AOKA-type pairings, as discussed below.

B. Spontaneous current and magnetic field

In Fig. 2(a), we plot the spontaneous current $j_{\hat{e}}(\mathbf{r})$ around the impurity. The current circles around the impurity, and the staggered current spreads toward the diagonal direction. The current in the diagonal direction is larger in the MN case.

We show the internal magnetic field in Fig. 2(b). The spontaneous field at the impurity site is oriented to the $-z$

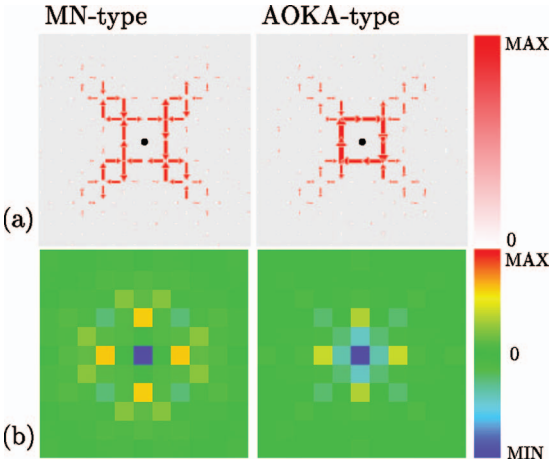

FIG. 2. (Color) (a) The spontaneous current $j_e(\mathbf{r})$ and (b) the internal magnetic field distribution $H(\mathbf{r})$ around a single impurity for the MN-type (left panels) and the AOKA-type (right panels) pairings. We show a region consisting of 11×11 sites with the impurity at the center. Solid circles in (a) indicate the impurity site.

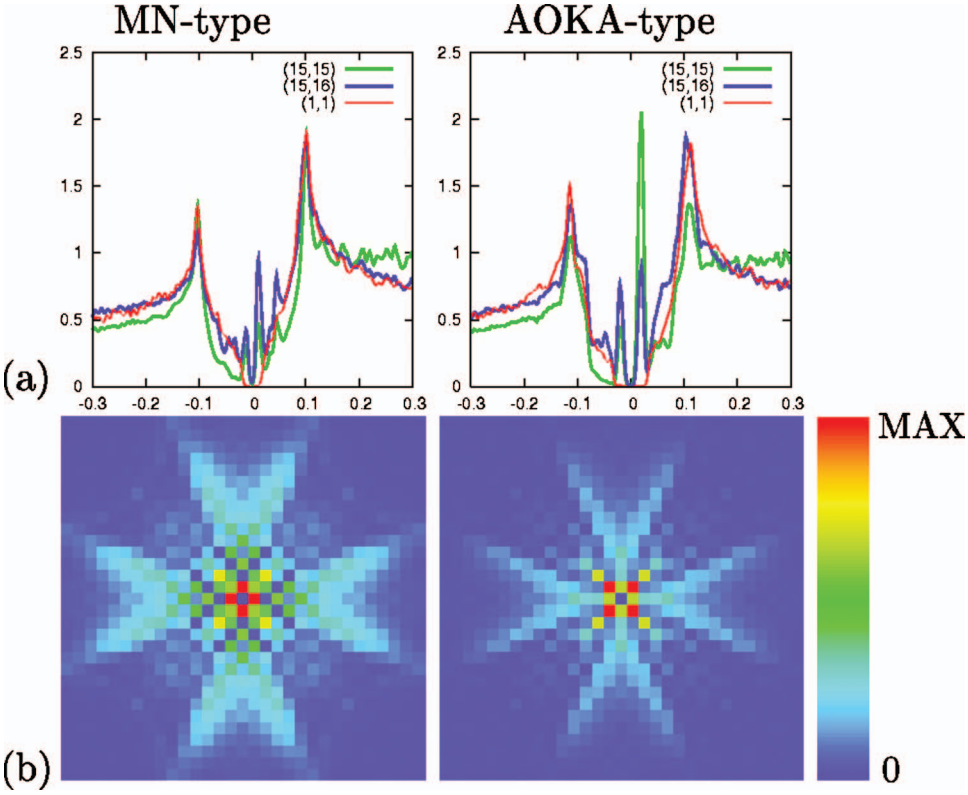

FIG. 3. (Color) (a) Spectrum of the LDOS $N(E,\mathbf{r})$ at sites (15,15), (15,16), and (1,1). (b) Density plot of the LDOS $N(E\sim 0,\mathbf{r})$ at the peak energy of the spectrum near $E\sim 0$ within a unit cell of 31×31 sites. The left and right panels are, respectively, for the MN-type and the AOKA-type pairings.

direction. This induced field is larger in the AOKA case, since the spontaneous current around the impurity is larger [Fig. 2(a)] due to the −6-winding of Δ_-' at the impurity [Fig. 1(c)]. To compensate for the spontaneous field at the impurity site, the spontaneous field is oriented toward the $+z$ direction near the impurity along the horizontal and vertical directions.

C. Local density of states

Figure 3(a) shows the LDOS $N(E,\mathbf{r}_i)$ around the impurity. We plot the $N(E,\mathbf{r}_i)$ at the nearest site $\mathbf{r}_i=(15,16)$, at the second nearest site (15,15), and at the farthest site (1,1). The energy spectrum of the uniform state with a p-wave anisotropic gap is reproduced at a site (1,1) far from an impurity. The asymmetry of $+E$ and $-E$ at a site (1,1) comes from the particle-hole asymmetry of the density of states (DOS) in the γ band with $t'=-0.4t$. Split LDOS peaks appear within the gap at (15,15) and (15,16) near the impurity. The side peak in the positive energy range is larger than that in the negative range for both pairings. When we compare the wave functions at the side peaks in the positive and negative energy ranges, the amplitude of the wave function in the positive energy range has a larger amplitude near the impurity. This difference may be related to the spontaneous current around the impurity.

In Fig. 3(a), the peak at (15,15) is larger (smaller) than that at (15,16) in AOKA-type (MN-type) pairing. The LDOS at this peak energy is shown in Fig. 3(b). The tail structure far from the impurity is similar, but the LDOS at nearest and second nearest sites is different between MN-type and AOKA-type pairings. In the case of AOKA-type (MN-type) pairing between diagonal (vertical) site quasiparticles, the low energy state is likely to appear in the diagonal (vertical) site next to the impurity site. The anisotropic gap structure on the Fermi surface also contributes to the difference of the LDOS. In the AOKA-type pairing, the gap amplitude has local minimum at [110] directions on the Fermi surface in addition to the minimum at [100] directions, as shown in Fig. 1 of Ref. 22.

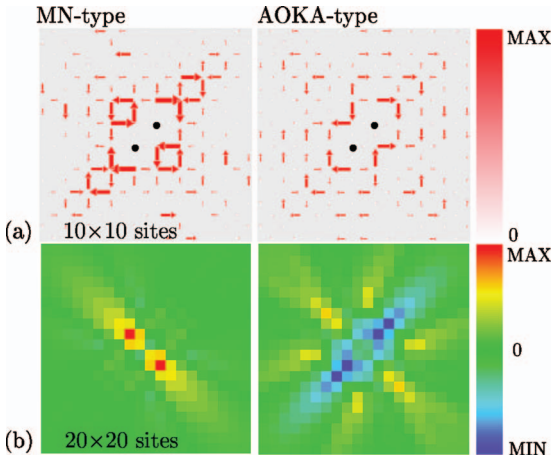

FIG. 4. (Color) (a) The spontaneous current $j_e(\mathbf{r})$ and (b) the internal magnetic field $H(\mathbf{r})$ for the MN-type (left panels), and the AOKA-type (right panels) pairings when a pair of impurities is situated in the diagonal direction. We show a region of 10×10 sites for (a) and a region of 20×20 sites for (b) around the impurities. Solid circles in (a) indicate the impurity sites.

IV. TWO IMPURITIES

As we have seen in Fig. 2(b), a drastic qualitative difference is not seen in the internal field between the two pairings in the case of single impurity. However, in the multiple impurity case, there are some cases producing qualitative differences between the two pairing cases in the spontaneous field distribution around the impurities due to the interference of the phase of the induced opposite chiral component [i.e., $\Delta_{-}(\mathbf{r})$ or $\Delta'_{-}(\mathbf{r})$ in Fig. 1]. As an example of this effect, we report the case when two impurities are located at next-nearest neighboring sites, i.e., sites (15,15) and (16,16) in our calculation. As in the single impurity case, the zero energy LDOS is large at the nearest site of the impurities for MN type, and at the next nearest site for AOKA type.

As shown in Fig. 4, the spontaneous current and the field distribution is not a simple summation of the distribution of the single impurity case, since the strong interference is at work between the two impurities. It is remarkable that for the MN-type pairing, the field intensity is strong in the direction perpendicular to the direction in which the impurities are aligned. The field orientation is toward the $+z$ direction in this case. On the other hand, in AOKA-type pairing, the spontaneous field, oriented toward the $-z$ direction, has a strong intensity in the direction parallel to the impurity alignment. This is a good example of the phenomena in which a difference in the phase windings of the pairing function on the Fermi surface results in experimentally observable quantities.

Therefore, it is valuable to experimentally examine the relation between the configurations of multi-impurities and the spontaneous magnetic field distribution around the impurities. This will be possible if we combine the STM and the field observation methods. By using STM, the configuration of impurities can be identified, and we expect the observation of the magnetic field distribution around the impurities. If we will scan the various configurations of impurities in $SrRuO_4$, we will obtain the relation of the impurity configurations and spontaneous field distribution, giving information for the pairing states.

V. SUMMARY

We have calculated, on the basis of the BdG equation, the spontaneous field and the electronic structure around the impurities in a spin-triplet chiral p-wave superconductor, where we compare the results between the MN-type pairing $\sin p_x + i \sin p_y$ and the AOKA-type pairing $\sin(p_x+p_y)+i\sin(-p_x+p_y)$.

We have shown that differences between the two pairings appear in the LDOS structure at the sites nearest and next nearest to the impurity site. Namely, the zero energy LDOS at the nearest site is found to be larger (smaller) than the LDOS at the second nearest site for MN-type (AOKA-type) pairing. When a pair of impurities is situated in the diagonal direction, the spontaneous magnetic field distribution around the impurities is quite different between the two pairings. The spontaneous field has a strong intensity along the line perpendicular (parallel) to the direction in which the two impurities are aligned in the MN-type (AOKA-type) pairing. We expect that the properties around the impurities shown here provide information for distinguishing the pairing state of Sr_2RuO_4.

The authors thank Y. Maeno, K. Ishida, H. Kontani, Y. Yanase, Y. Asano, H. Aoki, and R. Arita for valuable discussions. This work was supported by a Grant-in-Aid for the 21st Century COE "Frontiers of Computational Science" in Nagoya University and the 21st Century COE "Topology Science and Technology" in Hokkaido University.

*Electronic address: takigawa@topology.coe.hokudai.ac.jp

[1] Y. Maeno, H. Hashimoto, K. Yoshida, S. Nishizaki, T. Fujita, J. G. Bednorz, and F. Lichtenberg, Nature (London) **372**, 532 (2002).
[2] T. M. Rice and M. Sigrist, J. Phys.: Condens. Matter **7**, L643 (1995).
[3] R. Balian and N. R. Werthamer, Phys. Rev. **131** 1553 (1963).
[4] P. W. Anderson and P. Morel, Phys. Rev. **123** 1911 (1961).
[5] K. Ishida, H. Mukuda, Y. Kitaoka, K. Asayama, Z. Q. Mao, Y. Mori, and Y. Maeno, Nature (London) **396**, 658 (1998).
[6] J. A. Duffy, S. M. Hayden, Y. Maeno, Z. Mao, J. Kulda, and G. J. McIntyre, Phys. Rev. Lett. **85**, 5412 (2000).
[7] K. D. Nelson, Z. Q. Mao, Y. Maeno, and Y. Liu, Science **306**, 1151 (2004).
[8] Y. Asano, Y. Tanaka, M. Sigrist, and S. Kashiwaya, Phys. Rev. B **67**, 184505 (2003); Y. Asano, Y. Tanaka, M. Sigrist, and S. Kashiwaya, *ibid.* **71**, 214501 (2005).
[9] R. Jin, Y. Liu, Z. Mao, and Y. Maeno, Europhys. Lett. **51**, 341 (2000).
[10] C. Honerkamp and M. Sigrist, Prog. Theor. Phys. **100**, 53 (1998).
[11] M. Yamashiro, Y. Tanaka, and S. Kashiwaya, J. Phys. Soc. Jpn. **67**, 3364 (1998).
[12] G. M. Luke, Y. Fudamoto, K. M. Kojima, M. I. Larkin, J. Merrin, B. Nachumi, Y. J. Uemura, Y. Maeno, Z. Q. Mao, Y. Mori, H. Nakamura, and M. Sigrist, Nature (London) **394**, 558 (1998).
[13] Y. Tanaka and S. Kashiwaya, Phys. Rev. Lett. **74**, 3451 (1995); S. Kashiwaya and Y. Tanaka, Rep. Prog. Phys. **63**, 1641 (2000); M. Yamashiro, Y. Tanaka, and S. Kashiwaya, J. Phys. Soc. Jpn. **67**, 3364 (1998).
[14] Z. Q. Mao, K. D. Nelson, R. Jin, Y. Liu, and Y. Maeno, Phys. Rev. Lett. **87**, 037003 (2001); M. Kawamura, H. Yaguchi, N. Kikugawa, Y. Maeno, and H. Takayanagi, J. Phys. Soc. Jpn. **74** 531 (2005); F. Laube, G. Goll, H. v. Löhneysen, M. Fogelström, and F. Lichtenberg, Phys. Rev. Lett. **84**, 1595 (2000).
[15] K. Miyake and O. Narikiyo, Phys. Rev. Lett. **83**, 1423 (1999).
[16] T. Kuwabara and M. Ogata, Phys. Rev. Lett. **85**, 4586 (2000).
[17] R. Arita, S. Onari, K. Kuroki, and H. Aoki, Phys. Rev. Lett. **92**, 247006 (2004).
[18] T. Nomura and K. Yamada, J. Phys. Soc. Jpn. **69**, 3678 (2000).
[19] Y. Yanase and M. Ogata, J. Phys. Soc. Jpn. **72**, 673 (2003).

[20] Y. Hasegawa, K. Machida, and M. Ozaki, J. Phys. Soc. Jpn. **69**, 336 (2000).
[21] K. Deguchi, Z. Q. Mao, H. Yaguchi, and Y. Maeno, Phys. Rev. Lett. **92**, 047002 (2004); K. Deguchi, Z. Q. Mao, and Y. Maeno, J. Phys. Soc. Jpn. **73**, 1313 (2004).
[22] M. Takigawa, M. Ichioka, K. Machida, and M. Sigrist, Phys. Rev. B **65**, 014508 (2002).
[23] C. Lupien, S. K. Dutta, B. I. Barker, Y. Maeno, and J. C. Davis, cond-mat/0503317 (unpublished).
[24] M. I. Salkola, A. V. Balatsky, and J. R. Schrieffer, Phys. Rev. B **55**, 12648 (1997).
[25] H. Tsuchiura, Y. Tanaka, M. Ogata, and S. Kashiwaya, Phys. Rev. Lett. **84**, 3165 (2000).
[26] A. V. Balatsky, I. Vekhter, and J.-X. Zhu, cond-mat/0411318 (unpublished)
[27] C. H. Choi and P. Muzikar, Phys. Rev. B **39**, 9664 (1989).
[28] Y. Okuno, J. Phys. Soc. Jpn. **69**, 858 (2000).